Bioorganic & Medicinal Chemistry 19 (2011) 1055–1061

Contents lists available at ScienceDirect

Bioorganic & Medicinal Chemistry

journal homepage: www.elsevier.com/locate/bmc

Functional in vivo imaging of cysteine cathepsin activity in murine model of inflammation

Dejan Caglič [a], Anja Globisch [b], Maik Kindermann [b], Ngee-Han Lim [c], Volker Jeske [b], Hans-Paul Juretschke [b], Eckart Bartnik [b], K. Ulrich Weithmann [b], Hideaki Nagase [c], Boris Turk [a], K. Ulrich Wendt [b,*]

[a] Jožef Stefan Institute, Department of Biochemistry and Molecular and Structural Biology, Jamova 39, 1000 Ljubljana, Slovenia
[b] Sanofi-Aventis Deutschland GmbH R&D Chemical, Analytical Sciences and R&D Thrombosis & Angiogenesis, Industriepark Höchst, 65926 Frankfurt, Germany
[c] Kennedy Institute of Rheumatology Division, Imperial College London, London W6 8LH, United Kingdom

ARTICLE INFO

Article history:
Received 23 July 2010
Revised 29 September 2010
Accepted 12 October 2010
Available online 19 October 2010

Keywords:
Solid-phase synthesis
Activity-based probe
Cysteine cathepsin
Zymosan
Inflammation
In vivo imaging

ABSTRACT

Near-infrared fluorophore (NIRF)-labeled imaging probes are becoming increasingly important in bio-molecular imaging applications, that is, in animal models for tumor imaging or inflammation studies. In this study we showed that the previously introduced chemical concept of 'Reverse Design' represents an efficient strategy for the generation of selective probes for cysteine proteases from chemically optimized protease inhibitors for investigations in proteomic lysates as well as for in vivo molecular imaging studies. The newly developed activity-based probe AW-091 was demonstrated to be highly selective for cathepsin S in vitro and proved useful in monitoring cysteine cathepsin activity in vivo, that is, in zymosan-induced mouse model of inflammation. AW-091 showed higher signal-to-background ratios at earlier time points than the commercially available polymer-based ProSense680 (VisEn Medical) and thus represents an efficient new tool for studying early proteolytic processes leading to various diseases, including inflammation, cancer, and rheumatoid arthritis. In addition, the fluorescent signal originating from the cleaved AW-091 was shown to be reduced by the administration of an anti-inflammatory drug, dexamethasone and by the cathepsin inhibitor E-64, providing a valuable system for the evaluation of small-molecule inhibitors of cathepsins.

1. Introduction

The fields of activity-based proteomics and functional in vivo imaging both apply reactive chemical probes to detect enzymatic activities in native proteomic extracts, cells, and whole organisms. Because increased protease activity has been shown to be associated with a number of human diseases, including cancer, osteoarthritis, rheumatoid arthritis, much effort has been put into development of agents for monitoring of protease activity. Proteomic methods utilize activity-based probes (ABPs) which function as irreversible inhibitors, covalently modifying the catalytic site of target enzymes (covalent labeling ABPs) for the subsequent identification of specific enzyme proteomes from different physiological samples.[1] While such covalent labeling ABPs were originally designed to localize and identify activated enzymes in complex proteomic lysates, they have also been applied successfully to in vivo bio-imaging studies.[2,3] Nevertheless, monitoring the activity of low-abundant enzymes in vivo demands a different type of ABPs which are not irreversible inhibitors but substrates (substrate ABPs) and exhibit high specificity towards the enzyme under investigation. Selectivity for a given protease is controlled by the peptide recognition sequence. While some proteases show a high degree of selectivity for a given sequence (aspartic acid at P_1 site of caspase), others show high promiscuity and thus represent difficult targets for selective substrates. As more than 500 proteases are encoded in the human genome, it remains challenging to control selectivity of substrate cleavage in vivo. To address the issue of selectivity of substrates for a subset of proteases, namely cysteine cathepsins, we recently proposed that substrate ABPs with high selectivity for cysteine cathepsins can be obtained by a straightforward chemical concept, which we referred to as 'Reverse Design' (Ref. 4). We utilized two chemically optimized cathepsin inhibitors to design selective and cell-permeable ABPs. This was

Abbreviations: ABP, activity-based probe; Boc, *tert*-butyloxycarbonyl; DIPEA, diisopropyl-ethyl amine; DMF, dimethylformamide; DMSO, dimethylsulfoxide; DTT, dithiothreitol; ESI-MS, electrospray ionization mass spectrometry; equiv, equivalents; Fmoc, 9-fluorenylmethoxycarbonyl; HBTU, *O*-benzotriazole-*N*,*N*,*N*′,*N*′-tetramethyluronium hexafluorophosphate; HEPES, 4-(2-hydroxyethyl)-1-piperazineethanesulfonic acid; HOBt, *N*-hydroxybenzotriazole; HPLC, high performance liquid chromatography; LC–MS, liquid chromatography–mass spectrometry; NMR, nuclear magnetic resonance; PBS, phosphate buffered saline; RT, room temperature; TFA, trifluoroacetic acid; SPPS, solid-phase peptide synthesis.

* Corresponding author. Fax: +49 69 305 80169.
E-mail address: ulrich.wendt@sanofi-aventis.com (K.U. Wendt).

0968-0896/$ - see front matter © 2010 Published by Elsevier Ltd.
doi:10.1016/j.bmc.2010.10.028

achieved by converting their substrate-mimicking warheads into cleavable peptide bonds and subsequently attaching appropriate reporter groups. The selectivity profile of the inhibitors was thus transferred to the corresponding ABPs. Here we expand these studies in order to investigate whether 'Reverse Design' as a chemical concept is applicable to near-infrared (NIR) quenched fluorescent in vivo ABPs.

Cathepsins belong to a family of cysteine proteases, the majority of which reside in the endosomal/lysosomal system and are thus termed lysosomal cysteine cathepsins. There are 11 members present in humans, including cathepsins B, C, F, H, K, L, O, S, V, W, and X (Ref. 5). Cysteine cathepsins were long believed to be primarily involved in intracellular protein turnover, but a growing body of evidence suggests that at least some of them are involved in specific cellular processes as well as in numerous pathologies including cancer, cardiovascular diseases, osteoarthritis, rheumatoid arthritis, and other diseases linked with the immune system.[5] Cathepsin S, a potent cysteine peptidase, has been recognized to be the critical enzyme in invariant chain degradation, and antigen processing and presentation.[6] The enzyme has recently been considered as a pharmacological target for immune disorders and inflammatory diseases, including rheumatoid arthritis, atherosclerosis, and myasthenia gravis.[7–10]

We describe here the development and application of AW-091, a near-infrared quenched fluorescent substrate ABP, that is cleaved efficiently by cathepsin S. A direct comparison with a commercially available cathepsin-selective polymer-based substrate ProSense680 has been performed. AW-091 was shown to give higher signal-to-noise ratios at earlier time points after probe injection and thus offered readouts at earlier time points after induction of inflammation than the ProSense680 substrate. Moreover, comparable activity ratios (i.e., ratio between the signal in ipsilateral and contralateral limbs) were observed, whereas our probe showed shorter residence time in the tissue, rendering it attractive for repeated frequent activity determinations. In vitro profiling of AW-091 on recombinant enzymes together with in vivo inhibition studies suggests that the fluorescent signal of cleaved AW-091 recorded in mice correlates with the activity of cathepsin S.

AW-091 enabled the monitoring of cathepsin S activity in vitro as well as in a mouse model of inflammatory paw edema. The probe thus represents a promising tool for experimental investigation of inflammation pathophysiology and for monitoring efficacy of small-molecule inhibitors.

2. Material and methods

2.1. General material and methods

Unless otherwise noted, all reagents were purchased from commercial suppliers and used without further purification. Recombinant human cathepsins L and S were purchased from R&D Systems and cathepsin B from Sigma–Aldrich, whereas cathepsin K was produced as previously described.[11] Active protein concentrations were determined by active-site titration using E-64 (Peptide Institute). All solvents used were of HPLC grade. Reactions were analyzed by thin-layer chromatography on Merck 50 × 100 mm silica gel 60 aluminum sheets with fluorescent indicator or LC–MS. Column chromatography was carried out with Merck silica gel 60 (0.040–0.063 mm). Reverse-phase HPLC was performed on a C18 column Sun Fire (50 × 100 mm, Waters) or XBridge Prep C18 (5 μm, 10 × 100 mm, Waters). LC/MS data were acquired using the HP-Agilent 1100 MSD system. NMR-data were recorded on a Bruker DRX-400 system in d_6-DMSO and calibrated to the residual solvent peak.

2.2. General procedure for the solid-phase synthesis

The molecular scaffold **3** was synthesized using standard solid-phase peptide synthesis methods. The 2-chlorotrityl-chloride resin (Novabiochem, loading 1.4 mmol/g) was used as solid support. For loading of the resin (100 mg, 0.14 mmol) 2 equiv Fmoc-protected amino acid and 3 equiv DIPEA (74 μl, 0.42 mmol) were dissolved in 2 ml CH_2Cl_2 and the reaction mixture was added to the resin. The reaction mixture was shaken overnight at room temperature. The resin was washed three times with 2 ml CH_2Cl_2 and 2 ml DMF. For Fmoc-deprotection the resin was treated two times for 15 min with 2 ml 30% piperidine/DMF. A standard protocol was used for solid-phase peptide synthesis: 4 equiv Fmoc-protected amino acid, 4 equiv HBTU (212 mg, 0.56 mmol), 4 equiv HOBt (76 mg, 0.56 mmol), and 8 equiv DIPEA (196 μl, 1.12 mmol) were dissolved in 2 ml CH_2Cl_2/DMF (1/1; v/v). The reaction mixture was stirred 20 min at room temperature and then added to the resin. The reaction mixture was shaken for 2 h at room temperature.

For the cleavage of the peptide **3** from the solid-phase the resin was treated two times for 15 min with 2 ml 2% TFA/CH_2Cl_2 (v/v). The solvent was co-evaporated with toluene under reduced pressure and the product was purified by preparative HPLC (H_2O + 0.1% TFA; 10–95% CH_3CN, 15 min, 120 ml/min, column: Sun Fire 50 × 100 mm, Waters).

2.3. Synthesis of AW-091

AW-091 was synthesized following Scheme 1 with the fluorophore Cy7 and the quencher BHQ-3. ESI-MS: calculated: $[M+H]^+$ = 1620.0, found: $[M+H]^+$ = 1619.8.

2.4. Fluorescence assay for AW-091

For the in vitro enzyme activity assay, the active cathepsins were dissolved in AHNP-buffer (150 mM acetate/HEPES, pH 6.5, 300 mM NaCl; 0.001% Pluronic; 5–100 mM L-cysteine, depending on the enzyme) at a final concentration of 10 nM. The DMSO-dissolved AW-091 was added at 0.8–40 μM (final concentrations), followed by fluorescence measurements with a Tecan Safire2 plate reader (λ_{ex} = 710 nm, λ_{em} = 767 nm) at 25 °C. The final DMSO concentration in the assay did not exceed 1% (v/v). Steady-state kinetic data were fitted by non-linear least-squares regression analysis using the following relationship:

$$v = [S]V_{max}/(K_m + (1 + ([S]/K_{si}))[S]),$$

where v is the initial velocity, [S] the equilibrium concentration of substrate, V_{max} the maximal rate, K_m the Michaelis–Menten constant and K_{si} is the constant for substrate inhibition.

2.5. In vivo experiments with mice

2.5.1. Zymosan model

The animal study was performed according to the regulations of the German Animal Protection Law. Male CD-1 mice, 10 weeks of age, were obtained from Charles River Laboratories. Paw edema was induced by intraplantar injection of 10 μl of 10 mg/ml β-zymosan in sterile 0.9% NaCl-solution.

2.5.2. Administration of imaging agents, and treatments with dexamethasone and E-64

To study the effect of dexamethasone and E-64 on protease activity in inflamed paws, mice were distributed randomly into four groups (n = 3). One group was treated orally with dexamethasone (10 mg/kg) in vehicle (0.6% (w/v) methylcellulose–0.5% (v/v) Tween80) 1 day before zymosan, shortly after zymosan injection and 1 h before injecting AW-091. The second and third groups re-

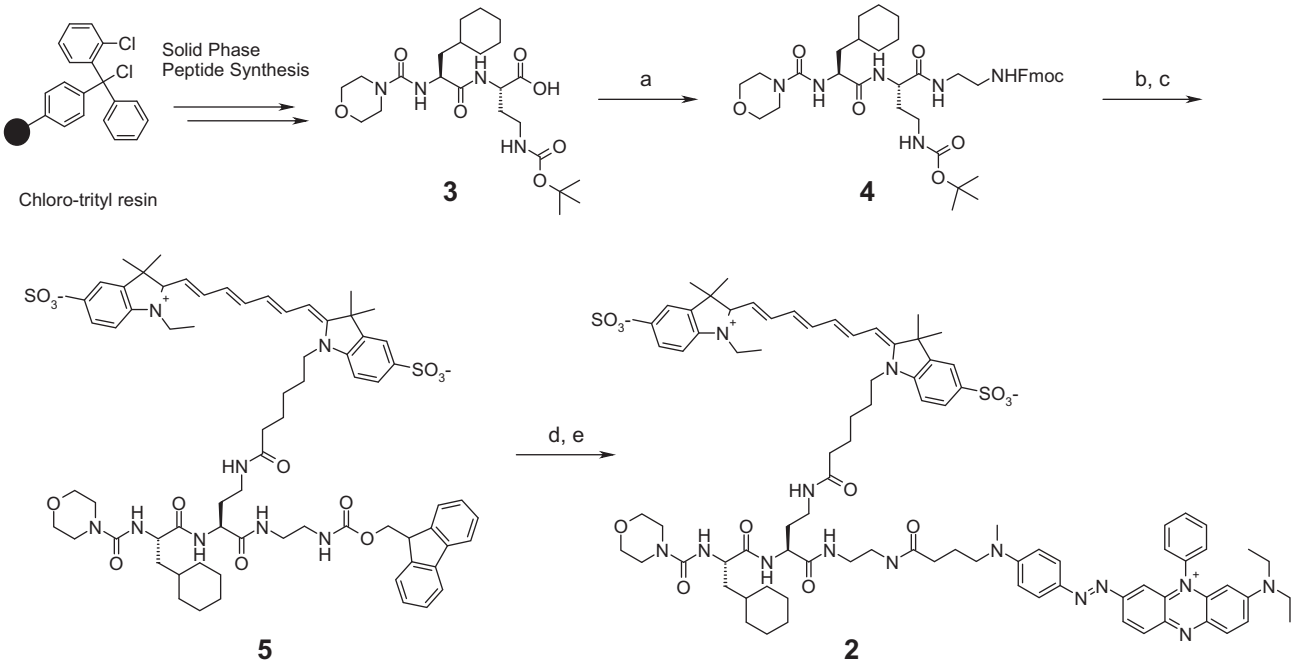

Scheme 1. Synthesis of AW-091 (molecule **2**) using a combination of solid-support and solution-phase synthesis as previously described (Ref. 4). Reagents and conditions: (a) 1.2 equiv HOBt, 1.3 equiv HBTU, 2 equiv *N*-Fmoc-ethane-1,2-diamine hydrochloride, 3 equiv DIPEA, DCM/DMF (1/1), 12 h; (b) 50% TFA/DCM, 10 min; (c) 1 equiv Cy7–OSu (GE Healthcare), 6 equiv DIPEA, DMF, 12 h; (d) Et_2NH/DMF (1/4), 30 min, rt; (e) 1 equiv BHQ-3–OSu (Biosearch Technologies), 6 equiv DIPEA, DMF, 12 h.

ceived four ip injections (2 days and 1 day before zymosan injection, shortly after zymosan injection and 1 h before injecting AW-091) of 10 and 30 mg/kg E-64 in 40% DMSO/PBS, respectively. For groups one to three, all mice were administered a 20 μM solution of AW-091 in PBS iv through tail vein injection (800 nmol/kg body weight of AW-091) 24 h after the zymosan injection. When animals ($n = 3$) were imaged with ProSense680 (VisEn Medical), 13.3 μM solution of the probe was administered iv through tail vein 24 h after zymosan treatment.

Because of the limited bioavailability of E-64, another control experiment was performed in the fourth group of animals. For these animals, zymosan, AW-091 and E-64 were injected directly into the foot pads ($n = 3$ for each group). Specifically, the right paws of 42-day-old C57BL/6 mice were injected with 30 μg of zymosan. After 2 days, 10 μl of 1 μM AW-091 with or without 1 μl of 1 mM E-64 was injected directly into ipsi- and contralateral paws of mice.

2.5.3. In vivo optical imaging and image analysis

NIRF in vivo imaging was performed with a Berthold Night Owl CCD imaging system with an excitation band-pass filter at 700/20 nm and an emission band-pass filter at 780/20 nm, or with a Kodak In Vivo FX Pro CCD imaging system with an excitation band-pass filter 710/20 nm and an emission band-pass filter at 790/20 nm emission filter. For imaging, the animals were anesthetized with 1.5–2% isofluran/N_2O/O_2. The animals were imaged in the supine position on a template ensuring a defined and reproducible position of the hind feet and care was taken to provide a uniform illumination at both positions of the feet. The tail and the upper portion of the body were covered with non-fluorescent plastic to obscure unspecific signals originating from the tail vein injection site, bladder, and liver. Throughout anesthesia and imaging, the body temperature of the mice was kept constant with heating pads and rectal measurement of their body temperature. Fluorescent images were taken at 10 min, 1, 3, 6, and 24 h after injection of the AW-091 using the Berthold system and every 3 min for 15 min at 0, 8, and 24 h after injection of the probe using the Kodak system. Fluorescence detection was performed with image acquisition times of 3 s or 2 min for the Berthold system and the Kodak system, respectively. Images were analyzed with Winlight 32 software version 2.93. Regions of interest (ROIs) were placed identically over the ipsi- and contralateral hind paws.

3. Results and discussion

The synthesis of quenched fluorescent activity-based probe AW-091 was based on previous findings that the selectivity profile of an optimized cathepsin inhibitor could be transferred into a selective and cell-permeable ABP by replacing the substrate-mimicking warhead of such an inhibitor by a cleavable peptide bond and subsequently attaching appropriate reporter groups for optical imaging.[4] Here we expand these studies in order to demonstrate that the chemical concept of *Reverse Design* is applicable to near-infrared (NIR) quenched fluorescent ABPs, suitable for in vivo bio-molecular imaging studies.

Crystal structures of cathepsin S suggested that the P_1 and P'_1 moieties are openly accessible to the surrounding solvent.[12,13] When compared to our previous cathepsins S probe (Ref. 4), two modifications have been applied here. In order to design a red-shifted NIR probe, we exchanged the positions of quencher and fluorophore in the P_1 and P'_1 position. This was mainly due to stability problems of the Cy7 fluorophore during the required deprotection conditions of the Boc-group. Furthermore, the composition of both linker groups in P_1 and P'_1 showed to have an influence on the performance of the probe. Especially unspecific cleavage could be reduced by changing the original lysine group in P_1 to the non-natural 2,4-diaminobutyric acid and from 2,4-diaminobutane in P'_1 to the shorter 1,2-diamino ethane. The cleavable peptide bond between the P_1 butyric acid derivative functionalized with the corresponding fluorophore Cy7 and the diamino ethane carrying the BHQ-3 quencher in P'_1 should be precisely oriented into the active site to be cleaved by cathepsin S.

The core scaffold of quenched fluorescent AW-091 (Fig. 1) was synthesized by standard solid-phase peptide chemistry followed by further derivatization of orthogonally protected amino groups in solution with Cy7 as a fluorophore and BHQ-3 as a quencher (for details see Reaction Scheme 1 and Supplementary Fig. S1). The core molecular scaffold, tripeptide **3**, was synthesized by conventional solid-phase peptide synthesis on chlorotrityl based resins by using Fmoc-protected amino-acid building blocks. Coupling of the Fmoc-mono protected 1,2-diaminoethane lead to the orthogonal protected building block **4**. First deprotection of the Boc-group and subsequent coupling to the Cy7–OSu ester led to intermediate **5** which after purification on a preparative HPLC was deprotected from the Fmoc group and a last coupling step with BHQ-3–OSu ester yielded AW-091 (molecule **2**).

In the first step, we set out to assess the efficiency of fluorescence quenching by comparing equimolar solutions (10 μM) of the free fluorescent dye Cy7 and of AW-091. The relative fluorescence intensities were 1: 0.22×10^{-3} (data not shown). Assuming similar brightness of the free fluorophores, this result suggests that AW-091 is efficiently quenched unless activated by enzymatic cleavage and thus represents a good in vivo imaging agent.

Enzymatic turnover and selectivity of AW-091 were tested in vitro against a panel of recombinant cysteine cathepsins (B, K, L, and S; see Fig. 2a). AW-091 exhibited good catalytic efficiency towards cathepsin S ($k_{cat} = 0.36\ s^{-1}$; $K_m = 2.5 \times 10^{-5}$ M) together with pronounced selectivity for cathepsin S in comparison to related cysteine cathepsins B, L, and K (k_{cat}/K_m for cathepsin S = $1.4 \times 10^4\ M^{-1}\ s^{-1}$, for cathepsin L = $1.9 \times 10^2\ M^{-1}\ s^{-1}$, no turnover detected for cathepsins B and K; see Fig. 2a). The kinetic properties of AW-091 show enhanced selectivity for cathepsin S over cathepsin L, another cysteine cathepsin involved in inflammation, as compared to our previous cathepsin-selective ABP 4 (see Table 1 and Ref. 4). Namely, the k_{cat}/K_m-value of AW-091 for cathepsin S is ~100-fold higher than for cathepsin L, whereas ABP 4 showed only ~2-fold preference for cathepsin S (Table 1). The results thus imply that the newly developed probe AW-091 is cathepsin S-selective and could be used to monitor cathepsin S activity in complex proteomic systems or in vivo models where activity of cathepsin S has been found to be upregulated.

Before testing the applicability of AW-091 in vivo, we wanted to rule out any proteolytic cleavages of AW-091 by unrelated families of proteases. Selectivity of AW-091 was therefore tested in vitro against cathepsins D and G, members of aspartic and serine protease families, respectively. As expected, none of the two non-cysteine cathepsins exhibited any proteolytic activity towards the probe (Fig. 2b). In addition, cross-reactivity of AW-091 towards metalloproteases was ruled out in a separate experiment using

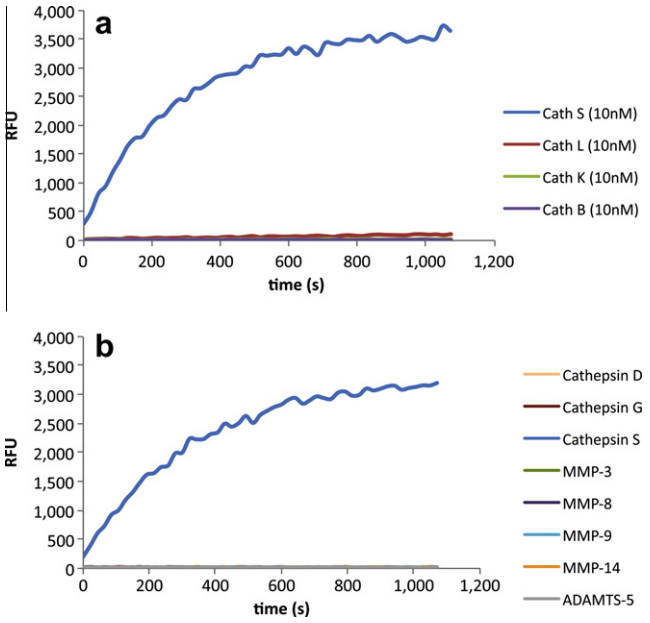

Figure 2. In vitro profiling of AW-091. (a) Recombinant cathepsins B, K, L, and S (10 nM final concentration) were incubated with 22.5 μM AW-091 and fluorescence was measured. Steady-state kinetic data were fitted by non-linear least-squares regression analysis. (b) In vitro selectivity of AW-091 towards other families of proteases. Recombinant enzymes (10–40 nM final concentration) were incubated with 60.0 μM AW-091 and fluorescence was measured. Cathepsin D belongs to the family of aspartic proteases, cathepsin G to serine proteases, cathepsin S is a cysteine proteases, whereas MMPs and ADAMTSs belong to the family of metalloproteases.

matrix metalloproteinase-3 (MMP-3), MMP-8, MMP-9, and MMP-14, which are involved in the degradation of the ECM in various pathologies including inflammation (reviewed in Ref. 14), as none of the MMPs cleaved the fluorescent probe (Fig. 2b). Collectively, these data demonstrated that AW-091 was cleaved preferentially by cathepsin S and only to a minor extent by cathepsin L, whereas unrelated serine cathepsin G and aspartic cathepsin D did not exhibit any activity towards the probe. Moreover, as none of the tested metalloproteases, which are involved in the pathogenesis of inflammation, cleaved AW-091, this probe could serve as a useful tool for in vivo imaging of cysteine cathepsin activity with minimal, if any, cross-reactivity with unrelated classes of proteases.

In vivo applicability of AW-091 was evaluated in a mouse model of inflammatory paw edema, introduced by unilateral, intraplan-

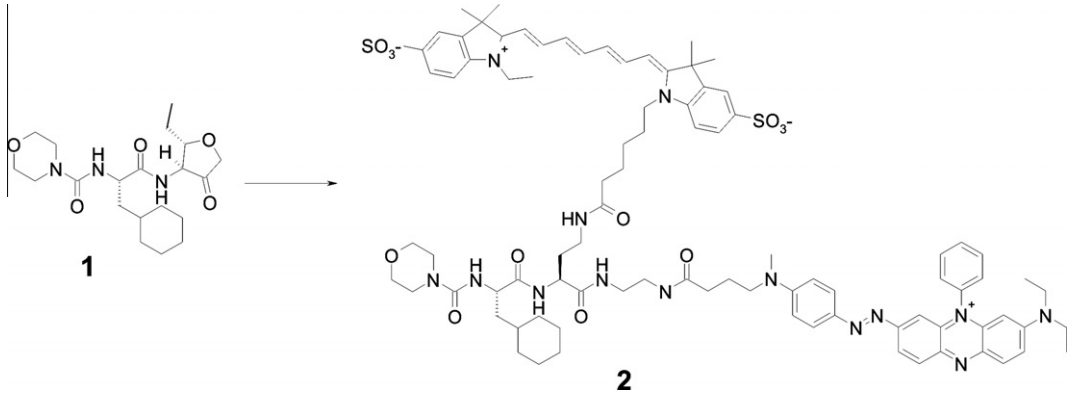

Figure 1. Conversion of the selective cathepsin inhibitor **1** into an activity-based probe AW-091 (molecule **2**) by the 'Reverse Design'. The quenched fluorescent probe is designed for in vivo studies containing Cy7 and BHQ-3 as fluorophore/quencher pair.

Table 1
Kinetic parameters of AW-091 and ABP 4 for related cysteine cathepsins[4]

		Cathepsin B	Cathepsin K	Cathepsin L	Cathepsin S
AW-091	K_m [M]	nd	nd	2.8×10^{-4}	2.5×10^{-5}
	k_{cat}/K_m [M^{-1} s^{-1}]	nd	nd	187	14,160
ABP 4	K_m [M]	3.2×10^{-3}	8.9×10^{-5}	8.4×10^{-4}	1.3×10^{-6}
	k_{cat}/K_m [M^{-1} s^{-1}]	332	187	7070	15,100

tar injection of zymosan.[15] Zymosan induces a rapid chronic inflammatory arthritis with mononuclear cell infiltration, synovial hypertrophy, and pannus formation. Joint swelling and infiltration of mononuclear cells appear already within 1 day after injection and subside within 14 days. Infiltration of immune cells in turn results in release of lysosomal enzymes and subsequent local increase in proteolytic activity.[15] In addition, expression and activity of cathepsin S, a protease with potent inflammatory activity, are known to be increased in various types of inflammatory arthritis.[10,16] Paw swelling in the ipsilateral hind paws was observed within hours after zymosan injection, while the contralateral paws served as controls. AW-091 was injected via tail vein and animals were imaged using a charge-coupled device (CCD) camera-based imaging system at various times after probe injection. Upon iv administration of the probe a differential fluorescence signal developed between ipsi- and contralateral paws (Fig. 3). A differential signal was evident as early as 10 min after probe application, reaching a ratio of 2–3 between ipsi- and contralateral paws already 1 h after probe application and remained above the signal in contralateral paws until 50 h after probe injection (Fig. 4a and c). Presence of BHQ-3 quencher group resulted in a low background signal (i.e., very low signal was observed in the contralateral paw).

Intensity, kinetics and tissue distribution of fluorescent signal generated by cleaved AW-091 was compared with a commercially available substrate ProSense680 (VisEn Medical). This substrate is a polymer-based reagent, where the relatively high density of loaded fluorophores onto the backbone structure leads to an internally quenched imaging agent.[17] Two groups of mice ($n = 3$), pretreated with zymosan, were imaged shortly after probe injection and at certain time intervals after injection. For AW-091 a differential signal between ipsi- and contralateral paws (ratio ipsi/contra) was observed as early as 10 min after AW-091 application and peaked at ~180 min, whereas ProSense680 yielded the maximum differential signal only after 24 h (Fig. 4). This faster signal onset favors AW-091 over ProSense680 for faster imaging and more frequent activity determinations. However, overall signal recorded

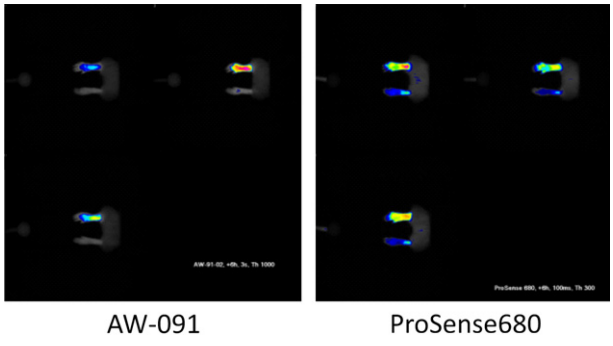

Figure 3. Optical imaging in a zymosan-induced paw inflammation mouse model. Signals from cleaved AW-091 and ProSense680 were compared using non-invasive NIRF in vivo imaging. Shown are colorimetric fluorescence images of the inflamed ipsilateral paws and the non-inflamed contralateral paws of three mice for each probe (tail and abdomen covered; images were taken 6 h after iv injection of the probe).

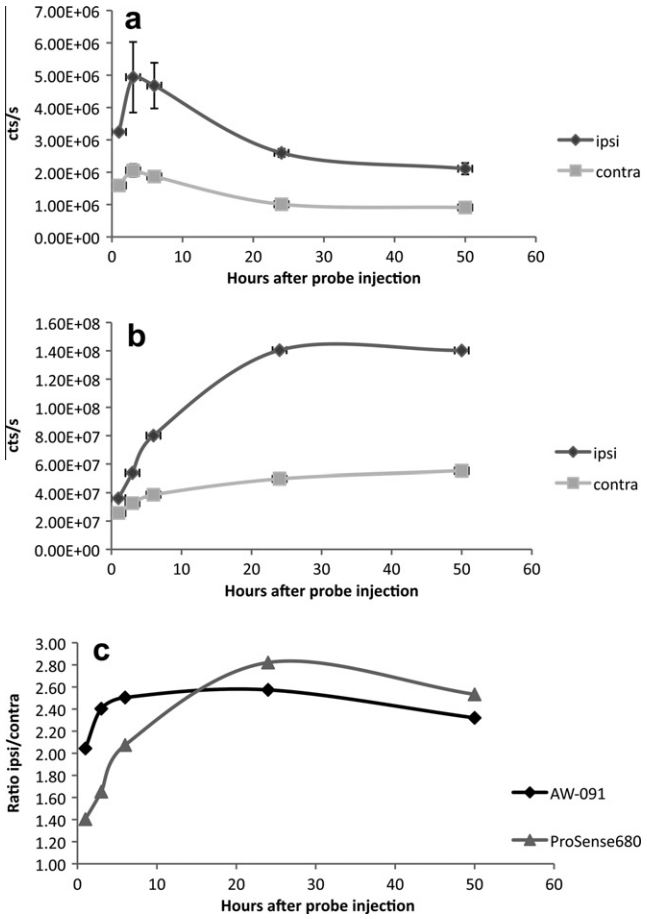

Figure 4. Quantification of paw fluorescence in mice treated with AW-091 and ProSense680. (a) 20 μM AW-091 was injected iv through tail vein. (b) 13.3 μM ProSense680 was injected iv through tail vein. Fluorescence (counts per second; cts/s) from inflamed ipsilateral and non-inflamed contralateral paws was measured at various time points after probe injection. Mean fluorescence and standard error is plotted relative to time after probe injection. Background levels were around 1.3×10^5 cts/s at all times. (c) Quantification of signal-to-background ratios expressed as ratios between fluorescent signals in ipsi- and contralateral paws for each time point.

in ProSense680-injected mice was more intense than signal from the cleaved AW-091 at all time points (see Fig. 4a and b for comparison). This higher signal probably stems from the higher density of fluorophores loaded onto the substrate backbone resulting in more intense fluorescence after cleavage by cathepsins and/or from the prolonged tissue retention of the polymer-based ProSense680 probe as compared to the smaller AW-091. ProSense680 substrate is cleaved by a range of cysteine cathepsins, including cathepsins B, K, L, S, aspartic cathepsin D, serine cathepsin G, and other proteases such as plasmin, urokinase plasminogen activator (uPA), CD10 and kallikrein-related peptidase 5 (http://www.visenmedical.com/products/fluorescence_agents/activatable/technical_support/index.html; information obtained from the VisEn Medical product datasheet), several of them involved in

inflammation (for review see Refs. 10,18–20), whereas AW-091 is preferentially cleaved by cathepsin S and exhibits no cleavage by proteases belonging to other families (Fig. 2).

In the next set of experiments, we chose to test if the anti-inflammatory agent dexamethasone could suppress inflammation and consequently reduce fluorescent signal originating from the cleavage of AW-091 in inflamed paw. Oral application of dexamethasone just before zymosan injection lowered the differential signal between ipsi- and contralateral paws significantly, demonstrating a downregulation of proteolytic activity in the inflamed paws (Fig. 5). As AW-091 was shown to be cleaved only by cysteine cathepsins, and not by other unrelated proteases, in vitro, we tested if the fluorescent signal in zymosan-injected paws could be suppressed by the general cysteine cathepsin inhibitor E-64. The inhibitor was applied intraperitoneally 2 days and 1 day before zymosan treatment, as well as during and after the treatment. Almost no inhibition was observed when low (10 μg/kg) or high concentration (30 μg/kg) of E-64 was used (Fig. 5). These data are in line with findings of Schurigt et al. who concluded that insignificant inhibition of cysteine cathepsins in mammary cancers and in lungs resulted from the poor pharmacokinetic properties of JPM-OEt, an E-64 derivative, and poor bioavailability when JPM-OEt was administered intraperitoneally.[21] Therefore, we decided to test a different type of administration, where E-64 and AW-091 were administered directly into the inflamed paw. This time, intraplantar injection of 1 μl 1 mM E-64 drastically decreased the signal of AW-091 (Fig. 6), suggesting that the observed fluorescent signal was indeed cathepsin-specific. The fluorescent signal from ipsilateral paw with injected E-64 ('ipsi + E-64' on Fig. 6) was significantly lower than the fluorescent signal from uninhibited inflamed paws ('ipsi' on Fig. 6) already 5 min after injection of the inhibitor and remained below the level from the uninhibited inflamed paw as long as 26 h after injection. The significant reduction of fluorescent signal by the cell-impermeable version of E-64 was anticipated as cathepsins are known to be the dominantly secreted enzymes in inflammation (for review see Ref. 10). Secreted cathepsins are thus expected to co-localize with E-64, which in turn efficiently inhibits their proteolytic activity. However, the fluorescent signal could be significantly reduced only when the inhibitor was administered directly into the inflamed paw, assuring that the inhibitor reached the site of the increased proteolytic activity.

In conclusion, an animal model was found to provide increased cysteine cathepsin activity which was successfully imaged with a newly developed and characterized activity-based probe AW-091. The imaged protease activity was localized in the foot pad around the site of zymosan injection. The fluorescent signal originating from the cleaved AW-091 was shown to be downregulated with dexamethasone, enabling the use of this model for compound testing. Intraplantarly-injected E-64 reduced the fluorescent signal, suggesting a significant portion of the fluorescent signal stemmed from cathepsin-mediated cleavage of AW-091. The ability to dynamically follow changes in proteolytic activity of cathepsin S suggests that AW-091 could be applied to monitor an inflammatory process in vivo and provides a model system for evaluation of small-molecule inhibitors against cathepsin S.

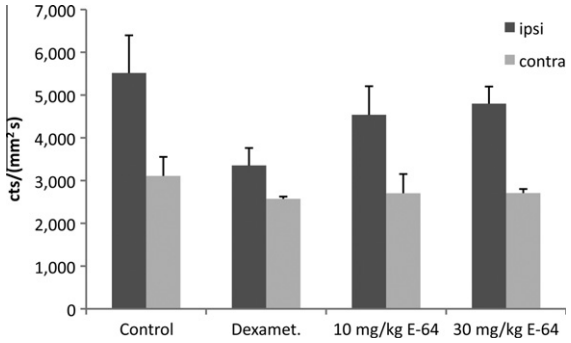

Figure 5. Dexamethasone reverted zymosan-induced inflammation in murine paws. Oral administration of 10 mg/kg dexamethasone (Dexamet.) prior to zymosan injections significantly suppressed the differential signal between ipsi- and contralateral paws. Intraperitoneal administration of 10 mg/kg or 30 mg/kg E-64 only slightly reduced the fluorescent signal in inflamed paws.

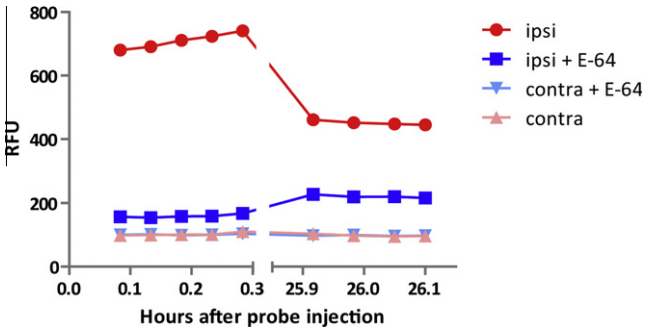

Figure 6. Intraplantar injection of E-64 significantly reduced fluorescent signal in inflamed paws. E-64 (1 μl of 1 mM solution) was injected directly into the inflamed paw and fluorescence from inflamed ipsilateral and non-inflamed contralateral paws was measured at various time points after probe injection.

4. Conclusions

Near-infrared fluorophore (NIRF)-labeled imaging probes are becoming increasingly important in bio-molecular imaging applications, that is, in animal models for tumor imaging or inflammation studies, due to the associated low auto-fluorescence of the surrounding tissue and deeper tissue penetration. The design of internally quenched protease probes allows imaging of enzyme activities in vitro or in vivo in real time and offers valuable information in monitoring and understanding the role of these enzymes in living systems. Not only activities and regulations but also specific inhibition of proteolytic enzymes by small molecules can now be made visible, providing new test modalities for medicinal chemistry research. The request for highly specific molecular imaging tools has prompted us to extend the design principle of such probes beyond peptide-based scaffolds and rather utilize the combination of chemically optimized protease inhibitors out of medicinal chemistry research together with data from structural biology for the design and synthesis of the presented fluorescent imaging activity-based probe AW-091.

In this study we show with newly developed AW-091 that the previously introduced chemical concept of 'Reverse Design' represents an efficient strategy for the generation of selective molecular probes for cysteine proteases using chemically optimized protease inhibitors. The concept thus allows the fine tuning of ABPs for activity-based investigations in proteomic lysates as well as for in vivo molecular imaging studies. Contrary to the known covalent labeling ABPs, 'Reverse Design' ABPs are substrates of the target enzyme. This property (i) renders them attractive for the monitoring of low-abundant enzymes and (ii) may provide a basis to ultimately establish quantitative (real time) investigations of the activity and inhibition of proteases in pharmacologically relevant in vivo models.

In specific, we demonstrate that AW-091 is highly selective for cathepsin S in vitro and proved useful in monitoring cysteine cathepsin activity in vivo, that is, in zymosan-induced mouse model of inflammation. AW-091 showed higher signal-to-background ratios at earlier time points than the commercially available polymer-based ProSense680 and thus represents an efficient new tool for studying proteolytic processes leading to various dis-

eases, including inflammation and rheumatoid arthritis. In addition, the fluorescent signal originating from the cleaved AW-091 was shown to be reduced by the administration of the anti-inflammatory drug dexamethasone and the cathepsin inhibitor E-64, providing a valuable system for evaluation of small-molecule inhibitors against cathepsin S.

Acknowledgements

This work was supported by the European Commission Framework 6 Program (CAMP project, LSHG-2006-018830) and the European Commission Framework 7 Program (FP7-Health-2009-241919-LIVIMODE project) and by the grant P1-040 from the Slovenian Research Agency to B.T. The authors declare no conflict of interest.

Supplementary data

Supplementary data (Supplementary Fig. S1 showing LC–MS spectrum of AW-091) associated with this article can be found in the online version, at doi:10.1016/j.bmc.2010.10.028.

References and notes

1. Evans, M. J.; Cravatt, B. F. *Chem. Rev.* **2006**, *106*, 3279.
2. Blum, G.; Mullins, S. R.; Keren, K.; Fonović, M.; Jedeszko, C.; Rice, M. J.; Sloane, B. F.; Bogyo, M. *Nat. Chem. Biol.* **2005**, *1*, 203.
3. Blum, G.; von Degenfeld, G.; Merchant, M. J.; Blau, H. M.; Bogyo, M. *Nat. Chem. Biol.* **2007**, *3*, 668.
4. Watzke, A.; Kosec, G.; Kindermann, M.; Jeske, V.; Nestler, H. P.; Turk, V.; Turk, B.; Wendt, K. U. *Angew. Chem., Int. Ed.* **2008**, *47*, 406.
5. Turk, B.; Turk, V. *J. Biol. Chem.* **2009**, *284*, 21783.
6. Nakagawa, T. Y.; Brissette, W. H.; Lira, P. D.; Griffiths, R. J.; Petrushova, N.; Stock, J.; McNeish, J. D.; Eastman, S. E.; Howard, E. D.; Clarke, S. R.; Rosloniec, E. F.; Elliott, E. A.; Rudensky, A. Y. *Immunity* **1999**, *10*, 207.
7. Link, J. O.; Zipfel, S. *Curr. Opin. Drug Discov. Devel.* **2006**, *9*, 471.
8. Riese, R. J.; Wolf, P. R.; Bromme, D.; Natkin, L. R.; Villadangos, J. A.; Ploegh, H. L.; Chapman, H. A. *Immunity* **1996**, *4*, 357.
9. Thurmond, R. L.; Sun, S.; Sehon, C. A.; Baker, S. M.; Cai, H.; Gu, Y.; Jiang, W.; Riley, J. P.; Williams, K. N.; Edwards, J. P.; Karlsson, L. *J. Pharmacol. Exp. Ther.* **2004**, *308*, 268.
10. Vasiljeva, O.; Reinheckel, T.; Peters, C.; Turk, D.; Turk, V.; Turk, B. *Curr. Pharm. Des.* **2007**, *13*, 387.
11. D'Alessio, K. J.; McQueney, M. S.; Brun, K. A.; Orsini, M. J.; Debouck, C. M. *Protein Expr. Purif.* **1999**, *15*, 213.
12. Pauly, T. A.; Sulea, T.; Ammirati, M.; Sivaraman, J.; Danley, D. E.; Griffor, M. C.; Kamath, A. V.; Wang, I. K.; Laird, E. R.; Seddon, A. P.; Menard, R.; Cygler, M.; Rath, V. L. *Biochemistry* **2003**, *42*, 3203.
13. Turkenburg, J. P.; Lamers, M. B.; Brzozowski, A. M.; Wright, L. M.; Hubbard, R. E.; Sturt, S. L.; Williams, D. H. *Acta Crystallogr., D Biol. Crystallogr.* **2002**, *58*, 451.
14. Tallant, C.; Marrero, A.; Gomis-Ruth, F. X. *Biochim. Biophys. Acta* **2010**, *1803*, 20.
15. Keystone, E. C.; Schorlemmer, H. U.; Pope, C.; Allison, A. C. *Arthritis Rheum.* **1977**, *20*, 1396.
16. Požgan, U.; Caglič, D.; Rozman, B.; Nagase, H.; Turk, V.; Turk, B. *Biol. Chem.* **2010**, *391*, 571.
17. Weissleder, R.; Tung, C. H.; Mahmood, U.; Bogdanov, A., Jr. *Nat. Biotechnol.* **1999**, *17*, 375.
18. Blasi, F.; Sidenius, N. *FEBS Lett.* **2010**, *584*, 1923.
19. Henke, P. K. *Vascular* **2007**, *15*, 366.
20. Heutinck, K. M.; ten Berge, I. J.; Hack, C. E.; Hamann, J.; Rowshani, A. T. *Mol. Immunol.* **2010**, *47*, 1943.
21. Schurigt, U.; Sevenich, L.; Vannier, C.; Gajda, M.; Schwinde, A.; Werner, F.; Stahl, A.; von Elverfeldt, D.; Becker, A. K.; Bogyo, M.; Peters, C.; Reinheckel, T. *Biol. Chem.* **2008**, *389*, 1067.